

# Sensing Contact Constraints in a Worm-like Robot by Detecting Load Anomalies

Akhil Kandhari<sup>1</sup>(✉), Andrew D. Horchler<sup>1</sup>, George S. Zucker<sup>1</sup>,  
Kathryn A. Daltorio<sup>1</sup>, Hillel J. Chiel<sup>2</sup>, and Roger D. Quinn<sup>1</sup>

<sup>1</sup> Department of Mechanical and Aerospace Engineering,  
Case Western Reserve University, Cleveland, OH 44106-7222, USA  
{axk751, rdq}@case.edu

<sup>2</sup> Departments of Biology, Neurosciences, and Biomedical Engineering,  
Case Western Reserve University, Cleveland, OH 44106-7080, USA  
hjc@case.edu

**Abstract.** In earthworms, traveling waves of body contraction and elongation result in soft body locomotion. This simple strategy is called peristaltic locomotion. To mimic this kind of locomotion, we developed a compliant modular worm-like robot. This robot uses a cable actuation system where the actuating cable acts like the circumferential muscle. When actuated, this circumferential cable contracts the segment diameter causing a similar effect to the contraction due to the circumferential muscles in earthworms. When the cable length is increased, the segment diameter increases due to restoring forces from structural compliance. When the robot comes in contact with an external constraint (e.g., inner walls of a pipe) continued cable extension results in both slack in the cable and inefficiency of locomotion. In this paper we discuss a probabilistic approach to detect slack in a cable. Using sample distributions over multiple trials and naïve Bayes classifier, we can detect anomalies in sampled data which indicate the presence of slack in the cable. Our training set included data samples from pipes of different diameters and flat surfaces. This algorithm detected slack within  $\pm 0.15$  ms of slack being introduced in the cable with a success rate of 75 %. We further our research in understanding reasons for failure of the algorithm and working towards improvements on our robot.

**Keywords:** Robot · Worm · Soft · Probability · Naïve Bayes · Cable · Actuation

## 1 Introduction

During the crawling movements of the earthworms, sensory feedback provides the animal with an ability to adapt to different types of environmental perturbations that may occur [16]. The importance of sensory feedback for maintaining rhythmic crawling motion has been established [7]. Mechanosensory organs and stretch, touch, and pressure receptors are the feedback sources in earthworms [15]. Due to the flexibility in the earthworm's body, it is unable to sense its posture from only stretch receptors [16]. However, the sensory input activities from the setae allows it to adapt to its environment and crawl smoothly on rough surfaces.

Many robots use cable actuation methods, like the Softworm [1–3], exoskeleton-type robots [19], cable-actuated parallel manipulators [8] and cable-suspended robots [18]. In our cable actuated robot, slack occurs in the cable when the robot comes in contact with an external constraint. It is undesirable as it reduces the efficiency during peristaltic locomotion. Detection of slack allows us to sense external constraints, which allows the robot to locomote efficiently. In this paper, our question is: can we recognize cable slack by searching for anomalies in feedback measurements from the actuators?

Anomaly detection techniques traditionally detect irregularities in new data after training on clean data [6]. Probabilistic approaches in predicting these anomalies have been studied widely [6, 13]. We use a probabilistic model to detect if slack has been introduced in our actuation cable to produce more efficient peristaltic locomotion [1] in our worm-like robot.

## 2 Slack Detection in a Cable-Actuated Robot

A significant issue faced when using cables is that they allow actuation in only one direction, i.e., a cable cannot be pushed. Initially, our Compliant Modular Mesh Worm (CMMWorm) robot had a bi-directional actuation system [9]. There were two sets of cables, one for circumferential actuation, (elongates the segment while making the diameter smaller) and one for longitudinal actuation (reduces segment length while increasing segment diameter). Due to nonlinear kinematics, the rate at which the longitudinal cables are spooled in is not equal to the rate at which the circumferential cables are spooled out. This difference in rates results in excess circumferential cable being spooled out. To prevent this excess cable from tangling or causing uneven wear, circumferential cable tensioning springs were required to keep the cable taut. Thus, cable slack was avoided, but as a result of the antagonistic cables, the design had high body stiffness.

For CMMWorm, Dynamixel MX-64T actuators are used. These actuators use PID (proportional-integral-derivative) control. Load feedback measures the torque applied by the actuator internally. We developed an open source library, DynamixelQ [12], for the OpenCM9.04 microcontroller used by CMMWorm for communication with AX and MX series Dynamixel actuators. It has been shown that the ability for a soft robot to respond to sensed load of its surroundings can permit efficient navigation, e.g., in narrowing pipes [4]. In the previous bi-directionally actuated iteration of CMMWorm [9], we used load measurements from the actuators to detect the walls of the pipe. Load measurements were sampled and then smoothed to filter noise using exponential smoothing. The data was then compared to a threshold value based on load data sampled. When a segment came in contact with the wall of a pipe the filtered load increased and exceeded the threshold. This allowed the algorithm to stop any further expansion of a segment.

In the current version of the CMMWorm (Fig. 1), only circumferential cables are used for actuation. The longitudinal cables have been replaced by six springs along the length of each segment such that, as the circumferential cable spools out, the springs passively return the segment to the maximum diameter allowed by the circumferential cable. In this simpler design, the spring stiffness need only be sufficient to restore the



**Fig. 1.** The six-segment Compliant Modular Mesh Worm (CMMWorm) robot crawling through a 20.3 cm inner diameter pipe. The linear springs that passively return the robot to its maximum diameter are visible along the length of each segment.

segments to their initial maximum diameter. The design is more robust, however, without the longitudinal cable, obstacle detection relies on detecting when the circumferential cable goes slack, rather than detecting an increase in longitudinal cable tension.

By reconfiguring the robot to use only one cable (circumferential), we can improve the mechanics of the motion (reducing cable friction losses, plastic deformation of the mesh, and limitations on range of motion), but detecting contact becomes a challenge. As the circumferential cable is pulled onto the spool, the diameter of a segment is constricted due to the length of cable available. In the other direction, when the cable is unspooled, the longitudinal springs expand the segment diameter as much as the increased cable length allows. However, when a segment comes in contact with an external constraint, such as that from the interior wall of a pipe, the segments stop expanding in proportion to the cable length that is unspooled and the cable can become slack. This causes reduced efficiency in responsive peristalsis that depends on accurate detection of contact [4]. Thus, a new way to control the segments of the robot was required.

It was observed that when the cable did experience slack, there was a small spike in the load values being recorded by the actuator. These load values are noisy and change based on the PID responses to cable tension. The small peaks due to slack can be thought of as anomalies in the load data being obtained. Hence, we approached this problem using a statistical probabilistic model. The problem then becomes to find the probability of slack occurring in the system given the load value that has been measured. If sampled values are not within the measured distribution, there is a higher probability that the segment has come in contact with an external force and the cable has gone slack.

### 3 Methods

When working with the robot, the actuators are configured to use a position control scheme. Position limits are specified and the actuator will rotate between these preset limits for a specified number of rotations (three rotations allow each segment to move

from maximum to minimum diameter). The actuators are run at their maximum speed and with no torque limits. Load measurements gathered from an actuator, although noisy, tend to spike when slack is introduced in the cable. This is analogous to lifting an object using a cable; if the cable is cut, a short jerk is felt due to the sudden change in tension. If it is possible to detect this spike within the noisy data, then it is possible to determine that the segment has come in contact against an external obstacle and should stop further expansion in order to avoid introducing slack.

To do so, a probabilistic approach is used to capture the occurrence of slack in each segment of CMMWorm by measuring the distribution of load values in the cases of slack and no slack. Load data is gathered from the actuators by expanding each segment in different diameter pipes and visually observing when the cable becomes slack. Slack is visually determined when the circumferential cable tensioning springs return to their equilibrium state. We then ensured that the segment was anchored against the walls of the pipe. Measurement of load values were continued after slack was introduced in order to collect data for the case of slack. The noisiness of the data and structural variability [10] leads to inconsistent training sets between segments. Due to nonlinear frictional properties, fraying of cables over time, and minor repairs being made over various runs, an individual segment also has variability in the load measurements recorded. This means that the distributions of load values (given slack or no slack) will be different for each segment and will change every time an adjustment is made to a segment.

To overcome this problem, we used a moving median filter for each actuator. Then the filtered median of the previous ten load measurements is subtracted from the current load measurement. This is referred to as the “relative median load” (RML). The absolute value of this difference is used such that the relative median load is always positive (Fig. 2). This helps filter variability in the range of load values among different segments, as well as within a segment, yielding a constant range of data for the entire robot.

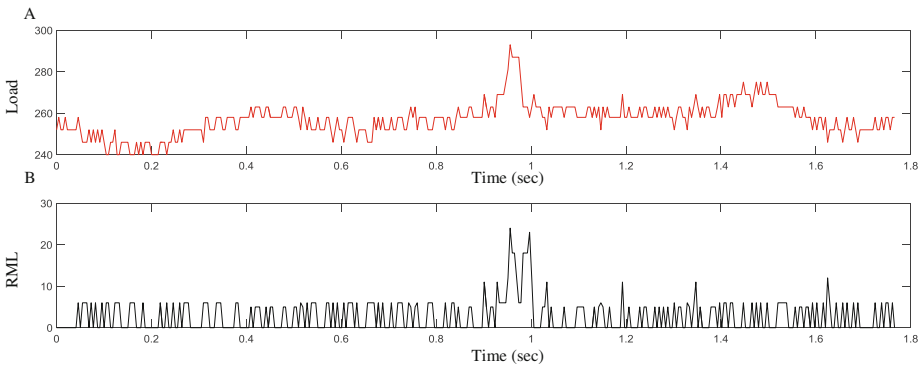


**Fig. 2.** (A) Load measurements from the actuator during expansion of a segment in a 20.3 cm inner diameter pipe. (B) The median filter measures the median of the previous ten load measurements. The output from this filter is then subtracted from the current load measurement. The absolute value of this is the relative median load (RML). This helps normalize the load data from different segments and use a single probability distribution for the entire robot. The spike in the above graphs at 0.95 s indicates that the cable has gone slack.

Based on the RML values, we build our distributions (Fig. 3). Data was gathered through ten runs for each of the six segments in 17.4 cm and 20.3 cm inner diameter pipes and on a flat surface. On flat surfaces the segments could expand to their maximum diameter without obstruction. Load values from these data sets were divided into two parts: load given slack in the cable and load given no slack in the cable. From these distributions it is observed that higher load values are more prominent when there is slack in the cable as compared to when there is no slack in the cable. Using naïve Bayes classification the possibility of slack occurring given a particular load value can be predicted based on probabilities,  $P$ , obtained from the training data.

The probability of a load measurement  $V_t$  at time  $t$  given slack in the cable,  $S$  is

$$P(V_t | S) = \frac{P(V_t)P(S | V_t)}{P(S)} \rightarrow P(S | V_t) = \frac{P(S)P(V_t | S)}{P(V_t)} \quad (1)$$

Similarly, the probability of a load measurement  $V_t$  at time  $t$  given no slack in the cable,  $\bar{S}$  is

$$P(V_t | \bar{S}) = \frac{P(V_t)P(\bar{S} | V_t)}{P(\bar{S})} \rightarrow P(\bar{S} | V_t) = \frac{P(\bar{S})P(V_t | \bar{S})}{P(V_t)} \quad (2)$$

Dividing (1) by (2), the ratio of likelihood of slack versus no slack given a particular load is

$$\frac{P(S | V_t)}{P(\bar{S} | V_t)} = \frac{P(S)P(V_t | S)}{P(\bar{S})P(V_t | \bar{S})} \quad (3)$$

To prevent the algorithm from identifying noise as slack, the previous five load measurements are used to find the product of probabilities of these measurements. This product is a ratio of probability of slack to no slack given a load value and is called the slack confidence (SC), where

$$SC = \prod_{i=0}^4 \frac{P(S)P(V_{t-i} | S)}{P(\bar{S})P(V_{t-i} | \bar{S})} \quad (4)$$

This helps not classify a noisy measurement for slack. Since the SC can be a large value, its natural logarithm,  $\ln(SC)$ , is used for plotting purposes throughout this paper. Through testing it was found that it took at least five probability values to localize a peak caused by slack in the cable.

A peristaltic controller needs to coordinate the simultaneous expansion and contraction of segments in order to minimize slip. At any given point, there are two active segments, one contracting and the other expanding in diameter. In between the two active segments there is a contracted inactive segment referred to as the “spacer segment” [10]. The remaining three inactive segments are expanded to the permissible limit and help in anchoring.

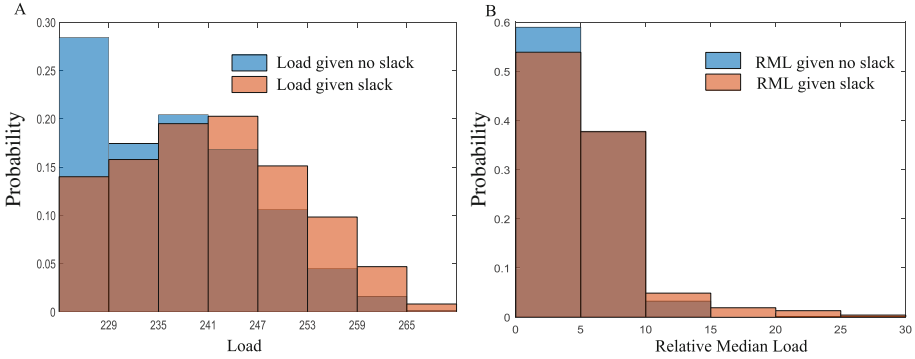


**Fig. 3.** Distributions showing the probability of load measurements (A) and relative median load measurements (RML) (B) given no cable slack (blue) and given cable slack (orange). The distributions show that the probability of obtaining higher load values decreases when there is no slack in the cable and the probability of obtaining higher load values increases when there is slack in the cable. The same trend is observed in the RML values. The RML distributions (B) are used to calculate slack confidence (SC) on the microcontroller by assigning probabilities to the load values obtained from the actuators. (Color figure online)

Once the wave is initiated, load measurements are recorded from the expanding segment after 150 ms to ignore transients that occur when the actuator starts from rest. After the actuator stabilizes, load measurements are recorded from the actuator of the expanding segment at 200 Hz. The slack confidence (SC) is then calculated by the microcontroller using Eq. (4). When slack occurs the SC has a large value compared to when there is no slack in the cable. At this point a distinct peak is observed (Fig. 4) and expansion of the segment is stopped and the control transitions to the next expanding segment. The wave travels down the length of the robot repeating the algorithm in each expanding segment. For the contracting segments a preset minimum position allows it to return to its initial configuration.

### 4 Results

Twenty runs each were done in 15.2 cm, 17.4 cm, and 20.32 cm inner diameter pipes and on a flat surface. The results shown in Table 1 summarize the success rate of slack being detected when the segment came in contact with the wall of the pipe or, in the

**Table 1.**  $N = 20$  runs each were done in 15.2 cm, 17.4 cm, and 20.3 cm inner diameter pipes and on a flat surface. The percentage of successful runs, false positive errors, and false negative errors for the four different cases is shown.

	Successful runs	False positive errors	False negative errors
15.2 cm Pipe	70 %	25 %	5 %
17.4 cm Pipe	70 %	20 %	10 %
20.3 cm Pipe	75 %	25 %	0 %
Flat surface	85 %	15 %	0 %

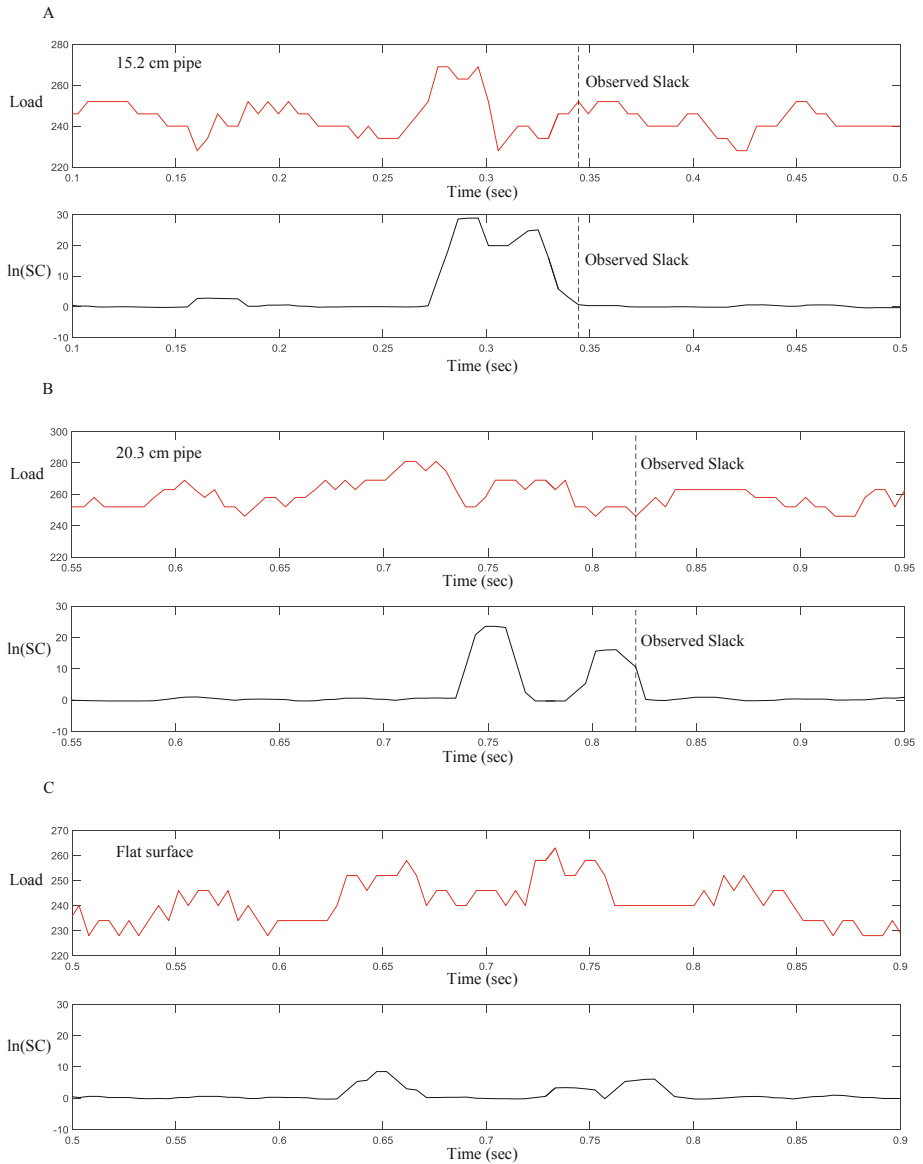


**Fig. 4.** Load measurements and natural logarithm of slack confidence,  $\ln(\text{SC})$ , from the actuator in three different cases, (A) 15.2 cm diameter pipe, (B) 20.32 cm diameter pipe, and (C) flat surface. In (A) and (B) the dashed vertical line depicts when slack is visually observed on the robot. The slack confidence has a significant peak ( $\ln(\text{SC}) > 10$ ) close to when slack is introduced in the cable in both cases. In (C), minor peaks are observed, but are not significant compared to when slack is introduced in the cable due to the walls of the pipe.

case of a flat surface, the absence of detection of slack throughout. Successful detection of slack is defined as when  $\ln(\text{SC}) > 10$  is detected within  $\pm 0.15$  s of coming in contact with the pipe (Fig. 4). Using this criterion, slack was detected successfully in 75 % of the tests. In pipes, 3.75 % of the tests showed a false negative, i.e., no significant peak was observed. At this point the cable would unspool even when the segment came in contact with an external barrier. The majority of the errors, 21.25 % of all the tests, were due to false positives, i.e., a significant peak occurred before the cable went slack. This would cause the robot to stop expansion before it came in contact with an external barrier. Thus a segment that should have been anchoring could slip relative to the pipe wall.

A detailed comparison between the load measurements and slack confidence for pipes of different diameters and on a flat surface is shown in Fig. 4. There is a lead time between when slack confidence peaks and when slack is visually observed in the cables. The lead time is less than 0.1 s. This difference might be due to the compliance of the mesh and the difficulty of precisely detecting slack visually (Fig. 5).

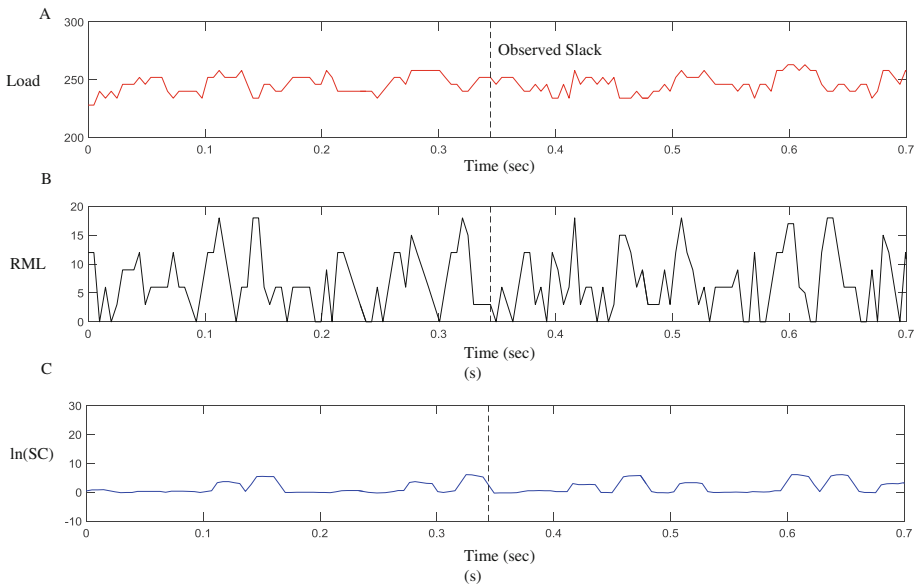


**Fig. 5.** Results from 15.2 cm diameter pipe indicating a false negative, i.e., the segment continued to expand even on coming in contact with the walls of the pipe. (A) Load measurement from the actuator, where no significant peak is observed. (B) The relative median load (RML) shows no significant peak throughout the test to quantify a point where slack is introduced. (C) The logarithm of SC shows a small spike when slack is introduced in the cable but it is not large enough to indicate that slack has been introduced.

False positive and false negative errors were observed in 25 % of runs. False positive errors cause inefficiency as it might cause the segment to slip. These errors might occur because of fraying of cables, high frictional loads on the cable, and



damaged components. False negative errors also cause inefficiency in the locomotion, as the robot is not able to adapt to its environment. False negative errors also cause excess cable being spooled out. This cable can get tangled with other components and might damage or break itself. This error might be due to the high amount of noise causing interference with the sampled data when slack occurs. False negative errors might also be an indication of plastic deformation of the mesh, where the loads are not uniformly transferred along the mesh of the segment.

## 5 Conclusions

The predictive model of detecting slack using probability distributions has allowed us to redesign our robot using a single cable for actuation. We can now detect slack in different diameter pipes along different segments using this algorithm. Using the sensory capabilities of our current actuators, we might be able to eliminate the need for additional sensors on the robot. Our future work will include achieving higher accuracy within a smaller time interval using a more dynamic method of predicting load measurements, such as Kalman filters [14]. There have also been studies on detecting anomalies using Dynamic Bayesian Networks [5, 13, 17]. We also want to apply a similar feedback algorithm in conjunction with dynamic oscillator networks, such as stable heteroclinic channels [4, 11] that could help achieve a more adaptive gait pattern.

Currently our robot can react to static environments, by controlling the expansion of each segment on coming in contact with an external constraint, but what if the environment was to change suddenly? If the robot slipped while locomoting, would it be able to adjust to such a change? In the future, the worm-like robot could continuously check for an external load and not just during expansion. In this way any change in the environment will trigger it to expand or contract in order to comply to its surroundings.

**Acknowledgements.** This work was supported by NSF research grant No. IIS-1065489. The authors would like to thank Dr. Soumya Ray and Kenneth Moses for their help during the course of this project.

## References

1. Boxerbaum, A.S., Chiel, H.J., Quinn, R.D.: A new theory and methods for creating peristaltic motion in a robotic platform. In: Proceedings of IEEE International Conference on Robotics and Automation, Anchorage, pp. 1221–1227 (2010)
2. Boxerbaum, A.S., Shaw, K.M., Chiel, H.J., Quinn, R.D.: Continuous wave peristaltic motion in a robot. *Int. J. Robot. Res.* **31**, 302–318 (2012)
3. Boxerbaum, A.S., Horchler, A.D., Shaw, K.M., Chiel, H.J., Quinn, R.D.: A controller for continuous wave peristaltic locomotion. In: Proceedings of IEEE International Conference on Intelligent Robots and Systems, San Francisco, pp. 197–202 (2011)

4. Daltorio, K.A., Boxerbaum, A.S., Horschler, A.D., Shaw, K.M., Chiel, H.J., Quinn, R.D.: Efficient worm-like locomotion: slip and control of soft-bodied peristaltic robots. *Bioinspir. Biomim.* **8**, 035003 (2013)
5. Dean, T., Kanazawa, K.: A model for reasoning about persistence and causation. *Comput. Intell.* **5**(3), 142–150 (1990)
6. Eskin, E.: Anomaly detection over noisy data using learned probability distributions. In: *Seventeenth International Conference on Machine Learning*, pp. 255–262 (2000)
7. Gray, J., Lissmann, J.W.: Locomotory reflexes in the earthworm. *J. Exp. Biol.* **15**, 5006–5017 (1938)
8. Hassan, M., Khajepour, A.: Analysis of bounded cable tensions in cable-actuated parallel manipulators. *IEEE Trans. Robot.* **27**(5), 891–900 (2011)
9. Horschler, A.D., Kandhari, A., Daltorio, K.A., Moses, K.C., Andersen, K.B., Bunnelle, H., Kershaw, J., Tavel, W.H., Bachmann, R.J., Chiel, H.J., Quinn, R.D.: Worm-like robotic locomotion with a compliant modular mesh. In: Wilson, S.P., Verschure, P.F., Mura, A., Prescott, T.J. (eds.) *Living Machines 2015*. LNCS, vol. 9222, pp. 26–37. Springer, Heidelberg (2015)
10. Horschler, A.D., Kandhari, A., Daltorio, K.A., Moses, K.C., Ryan, J.C., Stultz, K.A., Kanu, E.N., Andersen, K.B., Kershaw, J., Bachmann, R.J., Chiel, H.J., Quinn, R.D.: Peristaltic locomotion of a modular mesh-based worm robot: precision, compliance, and friction. *Soft Robotics* **2**(4), 135–145 (2015)
11. Horschler, A.D., Daltorio, K.A., Chiel, H.J., Quinn, R.D.: Designing responsive pattern generators: stable heteroclinic channel cycles for modeling and control. *Bioinspir. Biomim.* **10**(2), 026001 (2015)
12. Horschler, A.D.: DynamixelQ Library, version 1.2. <https://github.com/horschler/DynamixelQ>
13. Liang, K., Cao, F., Bai, Z., Renfrew, M., Cavusoglu, M.C., Podgurski, A, Ray, S.: Detection and prediction of adverse and anomalous events in medical robots. In: *Proceedings of Twenty-Fifth IAAI Conference*, pp. 1539–1544 (2013)
14. Manfredi, V., Mahadevan, S., Kurose, J.: Switching Kalman filters for prediction and tracking in an adaptive meteorological sensing network. In: *Proceedings of Second Annual IEEE Communications Society Conference on Sensor and AdHoc Communications and Networks (SECON)*, pp. 197–206 (2005)
15. Mill, P.J.: Recent developments in earthworm neurobiology. *Comp. Biochem. Physiol.* **12**, 107–115 (1982)
16. Mizutani, K., Shimoi, T., Ogawa, H., Kitamura, Y., Oka, K.: Modulation of motor patterns by sensory feedback during earthworm locomotion. *Neurosci. Res.* **48**(4), 457–462 (2004)
17. Pavlovic, V., Rehg, J.M., Murphy, K.P.: A dynamic Bayesian network approach to figure tracking using learned dynamic models. In: *Proceedings of the Seventh IEEE International Conference on Computer Vision*, vol. 1, pp. 94–101 (1999)
18. Roberts, R., Graham, T., Lippitt, T.: On the inverse kinematics, statics, and fault tolerance of cable-suspended robots. *J. Robot. Syst.* **15**(10), 581–597 (1998)
19. Veneman, J.F.: A series elastic- and Bowden-cable-based actuation system for use as torque actuator in exoskeleton-type robots. *Int. J. Robot. Res.* **25**(3), 261–281 (2006)